THE JOURNAL OF BIOLOGICAL CHEMISTRY VOL. 286, NO. 33, pp. 29192–29206, August 19, 2011

The Extracellular Regulated Kinase-1 (ERK1) Controls Regulated α-Secretase-mediated Processing, Promoter Transactivation, and mRNA Levels of the Cellular Prion Protein*

Received for publication, Decemeber 3, 2010, and in revised form, May 16, 2011 Published, JBC Papers in Press, May 17, 2011, DOI 10.1074/jbc.M110.208249

Moustapha Cissé[‡], Eric Duplan[‡1], Marie-Victoire Guillot-Sestier[‡1], Joaquim Rumigny[‡], Charlotte Bauer[‡], Gilles Pagès[§], Hans-Dieter Orzechowski[¶], Barbara E. Slack[‖], Frédéric Checler[‡2], and Bruno Vincent[‡3]

From the [‡]Institut de Pharmacologie Moléculaire et Cellulaire and Institut de Neuro-Médecine Moléculaire, Unité Mixte de Recherche, 6097 Centre National de la Recherche Scientifique/Université de Nice-Sophia-Antipolis, Equipe labellisée Fondation pour la Recherche Médicale, 660 route des lucioles, Sophia-Antipolis, 06560 Valbonne, France, the [§]Institute of Developmental Biology and Cancer, Unité Mixte de Recherche, 6543 Centre National de la Recherche Scientifique/Université de Nice-Sophia-Antipolis, Centre Antoine Lacassagne, 06189 Nice, France, the [¶]Institute of Clinical Pharmacology and Toxicology, Charité-Universitaetsmedizin Berlin, Campus Mitte, Luisenstrasse 10-11, 10117 Berlin, Germany, and the [‖]Boston University School of Medicine, Boston, Massachusetts 02118

The α-secretases A disintegrin and metalloprotease 10 (ADAM10) and ADAM17 trigger constitutive and regulated processing of the cellular prion protein (PrP^c) yielding N1 fragment. The latter depends on protein kinase C (PKC)-coupled M1/M3 muscarinic receptor activation and subsequent phosphorylation of ADAM17 on its intracytoplasmic threonine 735. Here we show that regulated PrP^c processing and ADAM17 phosphorylation and activation are controlled by the extracellular-regulated kinase-1/MAP-ERK kinase (ERK1/MEK) cascade. Thus, reductions of ERK1 or MEK activities by dominant-negative analogs, pharmacological inhibition, or genetic ablation all impair N1 secretion, whereas constitutively active proteins increase N1 recovery in the conditioned medium. Interestingly, we also observed an ERK1-mediated enhanced expression of PrP^c. We demonstrate that the ERK1-associated increase in PrP^c promoter transactivation and mRNA levels involve transcription factor AP-1 as a downstream effector. Altogether, our data identify ERK1 as an important regulator of PrP^c cellular homeostasis and indicate that this kinase exerts a dual control of PrP^c levels through transcriptional and post-transcriptional mechanisms.

The cellular prion protein is responsible for transmissible spongiform encephalopathies (TSE)[4] that can affect several mammals including humans (1). The common central event in prion pathologies is the conversion of the host-encoded cellular prion protein (PrP^c) into a pathogenic, insoluble, and partially protease-resistant isoform (PrP^{sc}) that aggregates and accumulates in specific brain areas, triggers neuronal degeneration, and ultimately leads to dementia and death (2).

Besides its implication in the development of TSE, it was postulated that PrP^c could fulfill physiological functions. Indeed, it has been suggested that PrP^c could participate in lymphocyte activation, cellular adhesion processes, neuronal growth, synaptogenesis, cellular signaling, and cell survival/apoptosis (for review, see Ref. 3).

The cellular prion protein is physiologically cleaved at the 111/112 peptidyl bond, thereby generating the so-called N1 amino-terminal fragment and its carboxyl-terminal membrane tethered counterpart named C1 (4). Interestingly, an additional cleavage occurring at the 90/91 peptide bond in Creutzfeldt-Jakob disease-affected brains yielding fragments referred to as N2 and C2 (4) preserves the 106–126 PrP^c domain. This peptide has been shown to be neurotoxic in *vitro* (5) and *in vivo* (6). Therefore, understanding the mechanisms underlying PrP^c processing could provide a means to interfere with PrP^c-dependent effects in both physiological and pathological conditions.

We and others previously established that PrP^c metabolism could be either constitutive or regulated by protein kinase C (PKC) (7) and that the disintegrins ADAM10 and ADAM17 were directly responsible for the constitutive and PKC-regulated processing of PrP^c, respectively (8, 9). Moreover, we demonstrated that ADAM9 acted as an upstream activator of ADAM10 activity (10). We very recently showed that stimulation of the M1/M3 muscarinic receptors with several classical or more receptor-specific agonists promotes isoform-specific PKC-dependent processing of the cellular prion protein via catalytic activation of ADAM17 upon phosphorylation on its threonine 735 (11, 12). Moreover, we demonstrated that the conventional PKCα, the novel PKCδ and PKCε, but not the atypical PKCζ isoforms participate in the PDBu- or carbachol-stimulated N1 production (12). Analysis of the amino acid sequence encompassing the intracytoplasmic Thr-735 of ADAM17 indi-

* This work was supported by the Fondation pour la Recherche Médicale and the Conseil Général des Alpes-Maritimes.

[1] Both authors equally contributed to this work.

[2] To whom correspondence may be addressed. Tel.: 33-4-93953460; Fax: 33-4-93957708; E-mail: checler@ipmc.cnrs.fr.

[3] To whom correspondence may be addressed: Institute of Molecular Biosciences, Mahidol University, Nakhon Pathom 73170, Thailand. Tel.: 66-0-2441-9003-7 (ext. 1451); Fax: 66-0-2441-1013; E-mail: mbbvc@mahidol.ac.th.

[4] The abbreviations used are: TSE, transmissible spongiform encephalopathies; PrP^c, cellular prion protein; CA, constitutively active; MEF, mouse embryonic fibroblasts; DN, dominant-negative; PDBu, phorbol ester 12,13-dibutyrate; Tricine, *N*-[2-hydroxy-1,1-bis(hydroxymethyl)ethyl]glycine.

cated that this residue is not part of the canonical (K/R)R(K/R/Q)GT(F/L/V)*X* consensus sequence that is required for phosphorylation by PKCα, -δ, or -ϵ isoforms, suggesting that PKC indirectly mediated phosphorylation of ADAM17 and thus, that N1 production required an additional kinase. Cautious analysis of mouse and human ADAM17 sequences revealed that the Thr-735 of ADAM17 was located in an APQTPG sequence corresponding to a canonical ERK1-targeted motif (*X*P*X*T P*X*).

We show here that ERK1 is absolutely required for PDBU- and carbachol-induced processing of PrP^c and that the inhibition of the ERK1 pathway totally impairs phosphorylation of ADAM17 on its Thr-735 and thereby, N1 production. In addition, we establish that, besides its crucial involvement in PrP^c-regulated processing, ERK1 modulates PrP^c protein and mRNA levels by a mechanism implying AP-1-dependent transcriptional control.

EXPERIMENTAL PROCEDURES

Antibodies and Pharmacological Agents—SAF32 is a monoclonal antibody raised against residues 79–92 of PrP^c (13) and was purchased from SPIBio (Montigny le Bretonneux, France). Anti-phosphothreonine polyclonal, anti-ERK1/2 (L34F12) monoclonal, and anti-phospho-ERK1/2 (197G2) polyclonal antibodies were from Cell Signaling Technology (Beverly, MA). Anti-β-tubulin and anti-β-actin monoclonal antibodies were purchased from Sigma. Anti-ADAM10 polyclonal antibody was purchased from U. S. Biological. Anti-ADAM9 (C-15) and anti-ADAM17 (H-300) polyclonal antibodies were from Santa Cruz Biotechnology (Santa Cruz, CA). Anti-HA monoclonal antibody (directed against amino acid residues 98–106 (YPYDVPDYA) of human influenza virus hemagglutinin) was from Covance (Berkeley, CA). BB3103 (hydroxamic acid-based zinc metalloprotease inhibitor) was kindly provided by British Biotech (Oxford, UK) and GF109203X was from Calbiochem (Fontenay-sous-bois, France). The fluorimetric substrate JMV2770 has been developed and characterized previously (14). Carbachol, phorbol ester 12,13-dibutyrate (PDBu), and the MEK inhibitor Uo126 were from Sigma. The Akt inhibitor LY294002 and the MEK inhibitor PD98059 were obtained from Cayman (VWR, Fontenay-sous-bois, France).

Cell Cultures, cDNA Constructs, and Transfections—Primary cultured neurons, 3F4MoPrP^c- and M1 receptor-overexpressing HEK293 cells (respectively, referred to as 3F4 and M1R cells throughout), were obtained and maintained in culture as previously described (7, 15, 16). Embryonic mouse fibroblasts (MEFs) (ADAM17$^{-/-}$, ERK1$^{-/-}$, and their respective wild-type controls) (17) were maintained in 50% F-12, 50% DMEM, 10% FCS. HA-tagged wild-type or dominant-negative (DN) forms of ERK1 (p44^{Mapk}), HA-tagged wild-type, constitutively active and dominant-negative forms of MEK1 (p45^{Mapkk}), ADAM17, and 3F4MoPrP^c cDNA constructs were previously described (18–22). Transient transfections in HEK293 cells and primary cultured neurons were carried out with Lipofectamine 2000 (Invitrogen), whereas fibroblasts were transiently transfected by means of the mouse embryonic fibroblasts Nucleofector™ kit (Amaxa Biosystems, Koeln, Germany) as described previously (23).

Western Blot Analysis—Cells were washed with phosphate-buffered saline (PBS) and resuspended in 300 μl of lysis buffer (10 mM Tris-HCl, pH 7.5, 150 mM NaCl, 0.5% Triton X-100, 0.5% deoxycholate, 5 mM EDTA) supplemented with a protease inhibitor mixture (Sigma). Protein concentrations were determined by the Bradford method (24) and 25 to 50 μg of proteins were separated by SDS-polyacrylamide gel electrophoresis on 8 (ADAM9, ADAM10, and ADAM17) or 12% (PrP^c, p53, p44/42, MEK, actin, and tubulin) Tris/glycine gels. Proteins were transferred onto nitrocellulose membranes (90 min, 100 V), blocked for 2 h in 5% nonfat milk, and incubated overnight at 4 °C with primary antibodies. Bound antibodies were detected using goat anti-mouse or goat anti-rabbit peroxidase-conjugated antibody (Beckman Coulter), and immunological complexes were revealed using ECL methods according to the manufacturer's instructions (Roche Applied Science). Chemiluminescence was recorded using a Luminescence Image Analyzer LAS-3000 (Raytest, Courbevoie, France) and quantification of captured images was performed using Image J Analyzer software.

Immunoprecipitation and Western Blot Analysis of N1—Cells cultured in 35-mm dishes were washed with PBS and incubated for 8 h at 37 °C in 1 ml of serum-depleted DMEM, in the absence (control) or presence of various pharmacological agents. Media were collected and supplemented with a protease inhibitor mixture and RIPA (0.1% SDS, 0.5% deoxycholate, 1% Nonidet P-40, pH 8), then incubated overnight with a 500-fold dilution of the monoclonal antibody SAF32 and protein A-Sepharose beads (Amersham Biosciences). Beads were washed twice with 500 μl of RIPA buffer, then once with 500 μl of PBS and submitted to SDS-polyacrylamide gel electrophoresis on a 16.5% Tris/Tricine gel. Two-hundred ng of purified recombinant N1 peptide obtained as previously described (11) were run on a separate lane as a standard. Proteins were transferred onto nitrocellulose membranes (45 min at 100 V) and incubated overnight at 4 °C with the monoclonal antibody SAF32 (dilution 1/2000). Immunological complexes were detected with a goat anti-mouse (dilution 1/2000) peroxidase-conjugated antibody (Beckman Coulter). Chemiluminescence was recorded using a Luminescence Image Analyzer LAS-3000 (Raytest) and N1 production was quantified using Image J analyzer software.

Detection of Threonine-phosphorylated ADAM17—M1R-HEK293 cells grown in 35-mm dishes were transiently transfected with ADAM17 cDNA. Twenty-four hours after transfection, cells were pre-treated for 1 h with various kinase inhibitors and then incubated for 15 min in fresh serum-free medium containing 1 μM PDBu, or 100 μM carbachol. Cells were then collected in 1 ml of lysis buffer (10 mM Tris-HCl, pH 7.5, 150 mM NaCl, 0.5% Triton X-100, 0.5% deoxycholate, 5 mM EDTA) supplemented with phosphatase inhibitor I and II mixtures and a protease inhibitor mixture (Sigma). Lysates were centrifuged (5 min at 13,000 $\times$ *g*) to remove insoluble material, then normalized for protein contents. One mg of proteins was supplemented with RIPA (0.1% SDS, 0.5% deoxycholate, 1% Nonidet P-40, pH 8) incubated overnight with immunoprecipitating anti-phosphothreonine antibody and protein A-Sepharose beads (Amersham Biosciences) (4 μg/1 mg of proteins). Immunoprecipitates were washed twice with 500 μl of RIPA buffer, then once with 500 μl of PBS and subjected to SDS-polyacryl-

amide gel electrophoresis on an 8% Tris/glycine gel. Proteins were transferred onto nitrocellulose membranes (2 h at 100 V) and incubated overnight at 4 °C with the polyclonal anti-ADAM17 antibody (dilution 1/1000). Immunological complexes were detected with a goat anti-rabbit peroxidase-conjugated antibody (dilution 1/5000) (Beckman Coulter) and revealed as described above.

Measurement of Endogenous ERK1/2 Phosphorylation—M1R-HEK293 cells grown in 35-mm dishes were pre-treated for 1 h with various kinase inhibitors and then incubated for 15 min in fresh serum-free medium containing 1 μM PDBu or 100 μM carbachol. Cells were then collected and treated as above. Lysates were centrifuged (5 min at 13,000 $\times$ *g*) to remove insoluble material, then normalized for protein contents. Fifty μg of proteins were separated by SDS-polyacrylamide gel electrophoresis on a 12% Tris/glycine gel. Proteins were transferred onto nitrocellulose membranes (75 min at 100 V), blocked for 2 h in 5% BSA, and incubated overnight at 4 °C with anti-phospho-ERK1/2 antibodies (dilution 1/1000 in 5% BSA). Immunological complexes were detected with a goat anti-rabbit peroxidase-conjugated antibody (dilution 1/5000 in 5% BSA) and revealed as described above.

Measurement of Disintegrin Activity—M1R-HEK293, mouse embryonic wild-type, and ERK1$^{-/-}$ fibroblasts were cultured in 6-well plates at 37 °C. At 80% of confluence, cells were pre-treated (or not) with the PKC inhibitor GF109203X (2 μM) or the MEK inhibitor Uo126 (10 μM) in the absence or presence of disintegrin inhibitor BB3103 (10 μM) for 1 h and incubated with 1 ml of PBS containing fluorimetric substrate JMV2770 (10 μM, (14)) with or without carbachol (100 μM) for various time periods at 37 °C. At each kinetic point, 100 μl of medium were taken out and substrate hydrolysis was fluorimetrically recorded (320 and 420 nm as excitation and emission wavelengths, respectively).

Mouse Brain Tissue Preparation—Brains from 7-week-old wild-type and ERK1$^{-/-}$ mice (17) were homogenized in lysis buffer (10 mM Tris-HCl, pH 7.5 containing 150 mM NaCl, 0.5% Triton X-100, 0.5% deoxycholate, 5 mM EDTA). Protein expressions were analyzed by Western blot as described above.

Measurements of PrP^c Promoter Transactivation—The 1543-bp 5′ promoter region of the human PrP^c gene or serial 5′-truncated constructs (1303-, 909-, 567-, 284-, and 131-bp constructs) were subcloned into the luciferase reporter vector pGL3 basic and used to measure PrP^c promoter transactivation, as extensively described (25). Cells grown in 12-well plates were co-transfected with full-length or mutant PrP^c promoter-luciferase, β-galactosidase (to normalize transfection efficiencies), and the indicated cDNAs with Lipofectamine (HEK293 cells) or with the Amaxa Nucleofector^{TM} kit (mouse embryonic fibroblasts). After a 36-h incubation in the presence of carbachol (100 μM), luciferase and β-galactosidase activities were measured with appropriate enzyme assay systems (Promega).

Site-directed Mutagenesis of PrP^c Promoter—A site-directed mutagenesis kit (QuikChange, Stratagene) was used following the manufacturer's instructions to convert the AP1-binding site nucleotide sequence TGACTCA (26) into TAAATCA. The two following sets of primers were purchased from Eurogentec: pPrPmut AP1-120S, 5′-CAACTCGTTTTTTCCGGTAAATCATTCCCGGCCCTGCTCG-3′ (forward primer) and pPrPmut AP1-120AS, 5′-CGAGCAGGGCCGGGAATGATTTACCGGAAAAAACGAGTTG-3′ (reverse primer). The altered nucleotides of the AP1 binding site are underlined. The construct was confirmed by sequencing.

Real-time Quantitative PCR—Total RNA was extracted and purified from mouse embryonic fibroblasts or HEK293 cells with the NucleoSpin® RNA II kit (Machery-Nagel, Hoerdt, France). Two μg of total RNA were reverse-transcribed using oligo(dT) priming and avian myeloblastosis virus reverse transcriptase (Promega). Real-time PCR was performed in an ABI PRISM 5700 sequence detector system (Applied Biosystems) using the SYBR Green detection protocol as outlined by the manufacturer. Specific primers for semi-quantitative or real-time PCR were designed using Primer Express software (Applied Biosystems) and were as follows: mouse PrP^c, forward, 5′-CTGCTGGCCCTCTTTGTGAC-3′ and reverse 5′-CTTTTTGCAGAGGCCGACAT-3′; human PrP^c, forward, 5′-AATCAAGCAGCACACGGTCA-3′ and reverse 5′-TCGGTGAAGTTCTCCCCCTT-3′.

Expression levels of human and mouse PrP^c genes were normalized by monitoring RNA levels of human GAPDH and mouse γ-actin genes, respectively, using the following primers: forward, 5′-TGGGCTACACTGAGCACCAG-3′ and reverse, 5′-CAGCGTCAAAGGTGGAGGAG-3′ for human GAPDH; forward, 5′-CACCATCGGTTGTTAGTTGCC-3′ and reverse, 5′-CAGGTGTCGATGCAAACGTT-3′ for mouse γ-actin.

Statistical Analysis—Statistical analyses were performed with the PRISM software (GraphPad, San Diego, CA) using the unpaired *t* test for pairwise comparisons.

RESULTS

Inhibitors of the MEK/ERK Pathway Block the PKC- and M1R-stimulated Processing of PrP^c and Prevent ADAM17 Phosphorylation on Its Threonine 735—In silico examination of human and mouse amino acid sequences of the ADAM17 cytoplasmic tail revealed that threonine 735, which had been shown to be selectively phosphorylated upon PKC-mediated M1/M3 muscarinic receptor activation (11), is embedded in an ERK1-specific consensus phosphorylation site (Fig. 1*A*). This prompted us to examine the effect of specific inhibitors of its upstream stimulating kinase MEK on regulated PrP^c processing. Fig. 1*B* shows that the PKC inhibitor GF109203X (27) and MEK inhibitor Uo126 (a phenylthiobutadiene that specifically inhibits MEK1 and MEK2, see Ref. 28) both impair the carbachol-stimulated increase of BB3103-sensitive JMV2770-hydrolyzing activity, a reporter assay for α-secretase/ADAM activity (14). Concomitantly, GF109203X and Uo126 abolish PDBu- and carbachol-stimulated N1 secretion in M1R HEK293 cells overexpressing PrP^c (Fig. 1*C*), whereas the Akt/PKB-specific inhibitor LY294002 remains inactive. None of the inhibitors affects PrP^c expression (Fig. 1*C*) or constitutive N1 production (Fig. 1*D*).

The above pharmacological data clearly linked PKC and muscarinic receptor stimulation to ERK1 and α-secretase activation. We therefore examined whether carbachol and PDBu stimulation could trigger ERK1 and ADAM17 phosphorylation in M1R HEK293 cells. Several lines of data indicate that it is

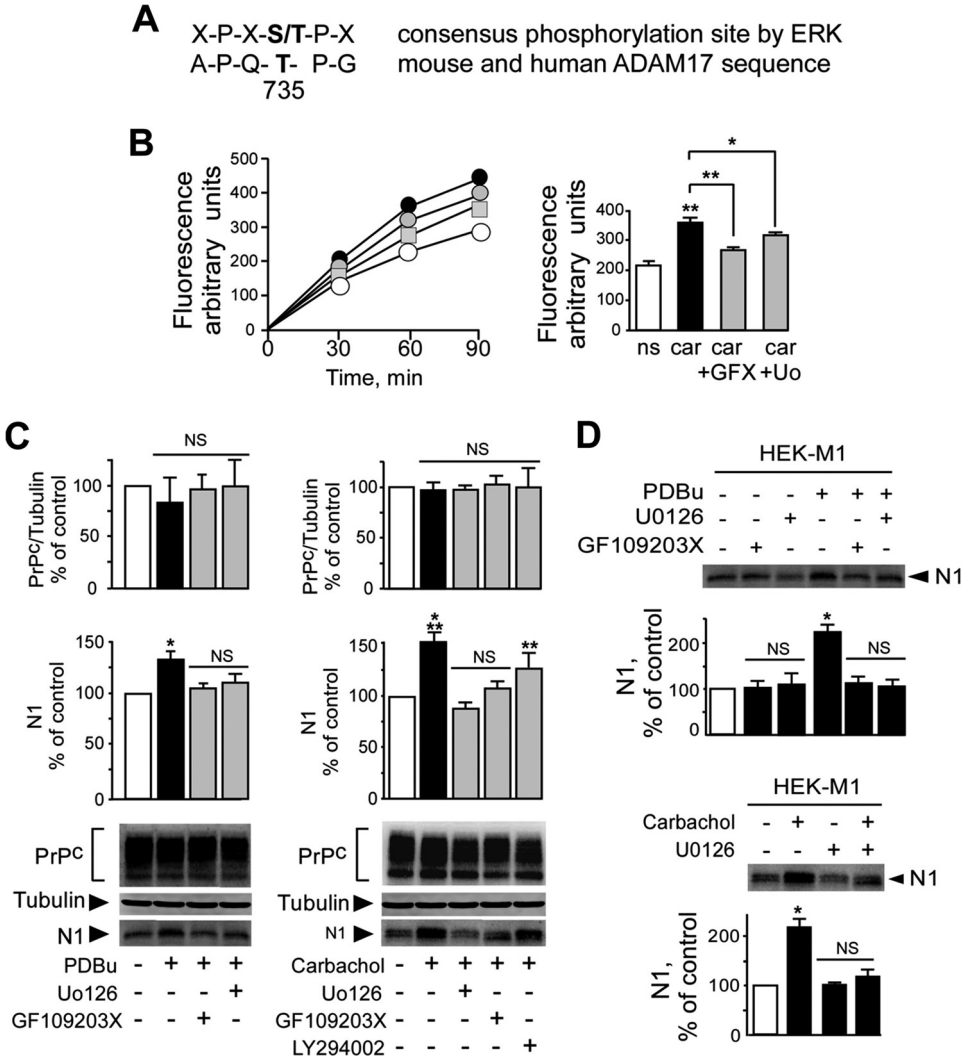

FIGURE 1. **Inhibitors of the ERK/MEK pathway impair PDBu- and carbachol-induced disintegrin activity and N1 recovery.** *A*, alignment of the consensus sequence required for ERK-mediated phosphorylation with amino acids surrounding the cytoplasmic threonine 735 of human and mouse ADAM17. *B*, cultured M1R-HEK293 cells were pretreated or not for 1 h with GF109203X (2 μM) or Uo126 (10 μM) and monitored for their BB3103-sensitive JMV2770-hydrolyzing activities in the absence or presence of carbachol (*Car*, 100 μM) as described under "Experimental Procedures." Aliquots of 100 μl were collected at the indicated times and fluorescence was recorded as described under "Experimental Procedures." A typical time course of BB3103-sensitive JMV2770 hydrolysis under various conditions is illustrated on the *left panel* and quantification is shown on the *right panel* (*white circles*, non-stimulated (ns); *black circles*, carbachol- (*carba*) stimulated; *gray squares*, carbachol + GFX109203X (*GFX*); *gray circles*, carbachol + U0126). Statistical analyses performed at 60 min (*right panel*) are the mean ± S.E. of three independent experiments. *, $p < 0.05$; **, $p < 0.001$. *C*, M1R-HEK293 cells grown in 35-mm dishes were transiently transfected with Mo3F4 PrP^c cDNA as described under "Experimental Procedures." Twenty-four hours after transfection, cells were pretreated (+) or not (−) for 1 h with the indicated inhibitors. Media were removed, and cells were incubated for 8 h in the absence (−) or presence (+) of PDBu (*left panel*) or carbachol (*right panel*). N1 content in conditioned medium as well as PrP^c and tubulin immunoreactivities in cell lysates were analyzed as described under "Experimental Procedures." *Bars* corresponding to the densitometric analyses are expressed as a percentage of control (non-stimulated cells) taken as 100 and represent the mean ± S.E. of six independent experiments. *, $p < 0.05$; **, $p < 0.005$; ***, $p < 0.0001$; *NS*, non-statistically significant. *D*, HEK-M1 cells were treated with the indicated inhibitors for 30 min. After removal of medium, cells were incubated for 8 h without (−) or with (+) PDBu (1 μM, *upper panel*) or carbachol (100 μM, *lower panel*) then constitutive or regulated N1 were monitored as described under "Experimental Procedures." *Bars* corresponding to the densitometric analyses of N1 are expressed as a percentage of control (non-stimulated cells in absence of inhibitors) taken as 100 and represent the mean ± S.E. of three independent experiments. *, $p < 0.0005$; *NS*, non-statistically significant.

indeed the case. First, a carbachol-induced phosphorylation of ERK1 is observed that is totally impaired by the MEK inhibitors PD098059 (29) and Uo126, the PKC blocker GF109203X but not by the Akt/PKB inhibitor LY294002 (Fig. 2*A*) without significantly altering endogenous levels of PrP^c- and ERK-like immunoreactivities (Fig. 2*A*, *lower panel*). Second, as is observed for ERK phosphorylation, muscarinic receptors and PKC stimulation by carbachol and PDBu trigger ADAM17 phosphorylation that was prevented by PD098059, Uo126, and GF109203X but not LY294002 (Fig. 2*B*). The strictly similar responsiveness of ERK and ADAM17 phosphorylation to the above selective pharmacological treatments suggested that muscarinic receptors and PKC stimulation yielding enhanced production of N1 indeed involves a downstream kinase effector, ERK, that ultimately potentiates ADAM17 phosphorylation and activity. Three lines of independent data confirmed this hypothesis. Thus, T735A mutation abolishes both carbachol and PDBu-stimulated N1 production in M1R-HEK293 cells (Fig. 3*A*) and prevents carbachol-induced N1 augmentation in cells expressing both ERK1 and M1R (Fig. 3*B*). Further-

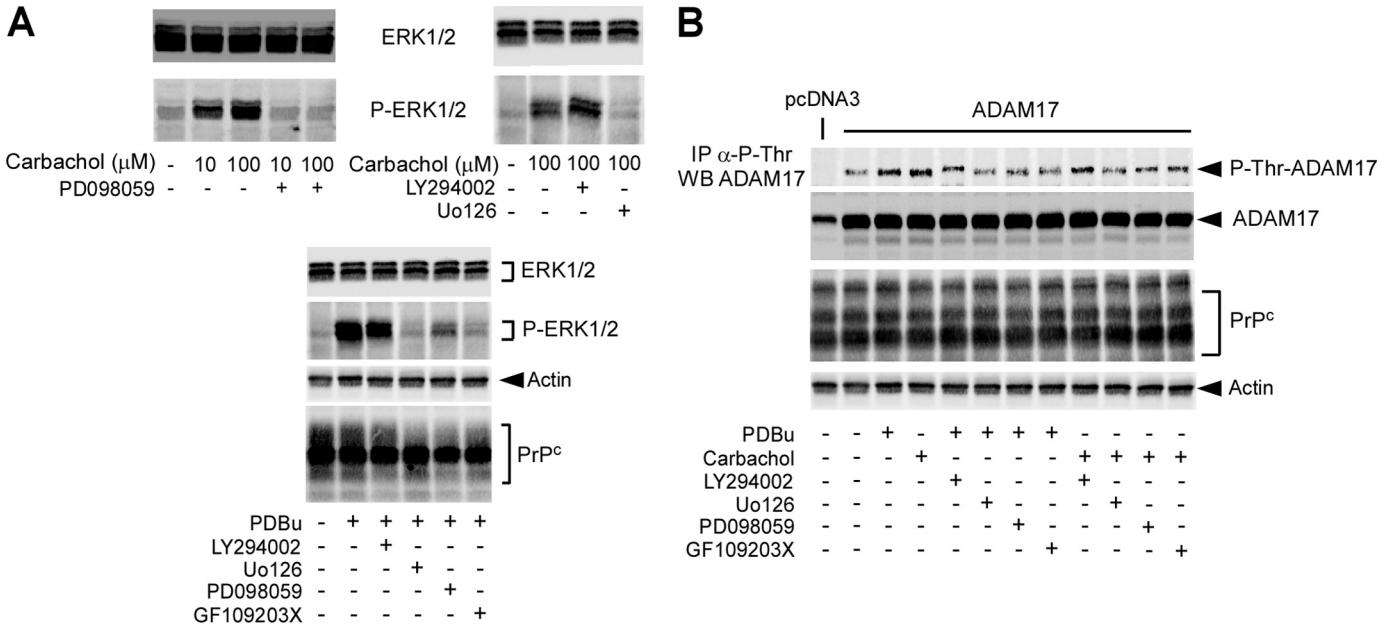

FIGURE 2. **Inhibitors of the ERK/MEK pathway prevent PDBu- and carbachol-dependent ADAM17 phosphorylation on its threonine residue.** *A*, M1R-HEK293 cells grown in 35-mm dishes were pretreated for 1 h without (−) or with (+) the indicated inhibitors (PD098059, 20 μM; LY294002, 5 μM; Uo126, 10 μM; GF109203X, 2 μM) and then incubated for 15 min with (+) or without (−) the indicated concentrations of carbachol (*upper panels*) or with PDBu (1 μM) (*lower panel*). Cells were collected, lysed as described under "Experimental Procedures," analyzed by 12% glycine SDS-PAGE and Western blotting using antibodies specifically directed against phospho-ERK1/2 (P-ERK1/2), total ERK1/2 (ERK1/2), PrP^c, or actin. *B*, M1R-HEK293 cells grown in 35-mm dishes were transiently transfected with empty pcDNA3 or ADAM17 cDNA. Twenty-four hours after transfection, cells were pre-treated for 1 h with inhibitors as in *A* and then stimulated (+) or not (−) with PDBu (1 μM) or carbachol (100 μM) for 15 min as indicated. Threonine-phosphorylated ADAM17 (*P-Thr-ADAM17*) was monitored by immunoprecipitation (*IP*) of 500 μg of proteins with a specific antibody directed against phosphothreonine and Western blotting with an ADAM17-specific antibody as described under "Experimental Procedures." Fifty μg of the same samples were then submitted to 8 (ADAM17) or 12% (PrP^c and actin) glycine SDS-PAGE and Western blotted with specific corresponding antibodies as described under "Experimental Procedures." All illustrations are typical data of three independent experiments.

more, the ADAM17 mutation fully blocks the CA-MEK-associated increase of N1 production (Fig. 3*C*). Altogether, these data clearly indicate that ERK1 indeed requires Thr-735-phosphorylable ADAM17 to stimulate N1 production.

Constitutive Activation or Reduction of MEK1 and ERK1 Modulate Carbachol- and PDBu-induced Processing of PrP^c in Human Cells and Mouse Primary Neurons—The above clues of a signaling pathway linking muscarinic receptors, PKC, ERK, and physiological processing of PrP^c based on pharmacological compounds with rather narrow specificity was further reinforced by a series of experiments aimed at more selectively modulating ERK1 and its activating kinase MEK1. Thus, we took advantage of the design of cDNAs encoding HA-tagged wild-type (WT), catalytically inactive dominant-negative forms of these two kinases (DN-MEK and DN-ERK) and a constitutively active form of MEK (CA-MEK). Dominant-negative forms of ERK1 and MEK were obtained by mutations (T192A and S222A, respectively) that abrogate their phosphorylation at regulatory sites (18, 19), whereas CA-MEK was obtained by replacing two serine residues involved in Raf1/MAPKKK-dependent regulatory phosphorylation of MEK1 by the negatively charged aspartate (S218D/S222D) (20). Wild-type ERK1 or MEK1 significantly increase carbachol-induced N1 secretion in PrP^c-transfected M1R HEK293 cells (Fig. 4*A*), whereas DN-ERK1 or DN-MEK1 expressions totally prevented carbachol (Fig. 4*A*) or PDBu (not shown) stimulated N1 production.

Expression of CA-MEK1 in M1R HEK293 cells transiently transfected with PrP^c is *per se* sufficient to trigger N1 secretion even in non-stimulated conditions (Fig. 4*B*). Furthermore, in carbachol-stimulated conditions, the treatment of mock-transfected M1R HEK293 cells with atropine inhibits the secretion of N1, whereas the secretion of N1 triggered by CA-MEK1 expression remains unaffected by atropine (Fig. 4*C*). These results indicate that blockade of endogenous muscarinic receptors do not interfere with the constitutively active MEK/ERK-associated N1 increase and therefore demonstrate that the MEK/ERK signal controlling N1 secretion occurs downstream to the muscarinic receptors. Interestingly, as expected, neither wild-type nor dominant-negative ERK1/MEK1 are able to modulate N1 production in 3F4 HEK293 cells that are devoid of endogenous muscarinic receptors (30) (Fig. 4*D*), confirming the importance of M1 receptors as essential mediators of PKC/ERK-dependent processing of PrP^c. The above results have been confirmed in primary cultured neurons. First, we establish that N1 production was also potentiated by carbachol and PDBu treatments in neurons (Fig. 5). Second, both DN-ERK1 and DN-MEK1 overexpressions restore endogenous levels of N1 produced by untreated cells with no apparent modification of PrP^c-like immunoreactivity (Fig. 5). Altogether, the above data indicate that the pathway described previously also occurs in a physiological neuronal cell system and, therefore, that this cascade was clearly not cell specific but likely ubiquitous.

ERK1 Deficiency Lowers PrP^c Expression—As anticipated from our previous data, genetic ablation of ERK1 drastically affects PrP^c processing. Thus, $ERK1^{-/-}$ MEFs prepared from ERK1 knock-out animals (17) secrete lower amounts of the N1 fragment than wild-type cells (Fig. 6*A*). ERK1 gene disruption also fully abolishes the PDBu- and carbachol-stimulated N1

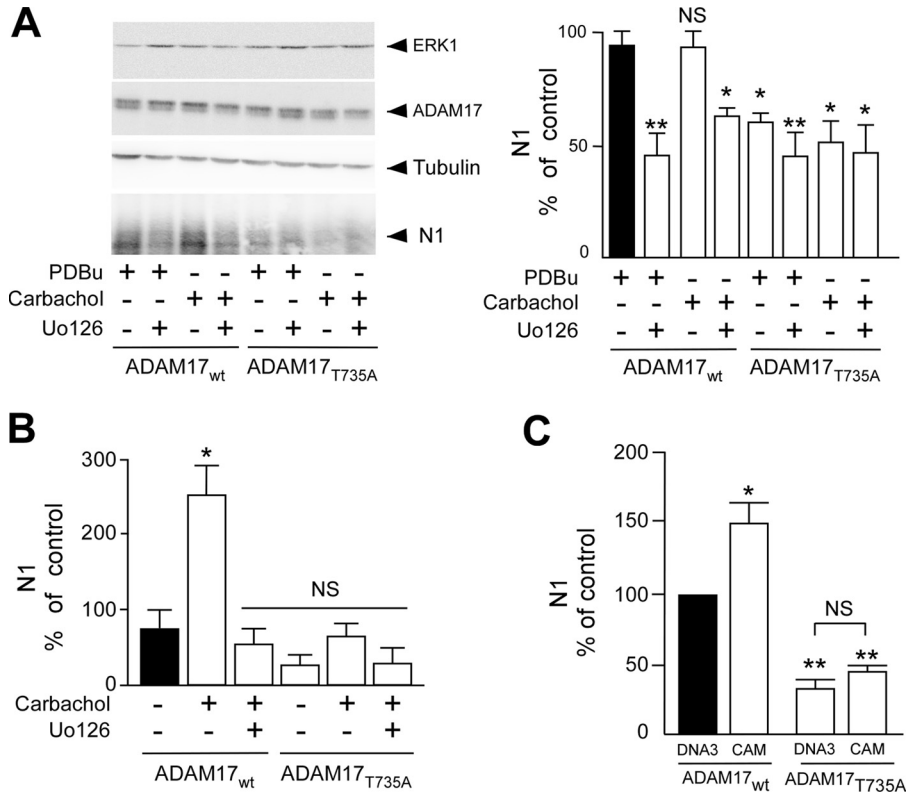

FIGURE 3. **Mutation of the threonine 735 of ADAM17 abolishes the ERK-1 dependent α-secretase cleavage of PrP^c.** *A*, M1R-HEK293 cells grown in 35-mm dishes were transiently transfected with Mo3F4 PrP^c, ERK1, and ADAM17$_{wt}$ or ADAM17$_{T735A}$ cDNAs as described under "Experimental Procedures." Twenty-four hours after transfection, cells were treated with (+) or without (−) PDBu (1 μM), carbachol (100 μM), and Uo126 (10 μM). Sixteen hours after treatment, *N1* content in conditioned media as well as ERK1, ADAM17, and tubulin immunoreactivities in cell lysates were analyzed as described under "Experimental Procedures." *Bars* corresponding to the densitometric analyses of N1 immunoprecipitation are expressed as a percentage of control (PDBu-stimulated ADAM17$_{wt}$-expressing cells, *black bar*) taken as 100 and represent the mean ± S.E. of five independent experiments. *, $p < 0.05$; **, $p < 0.001$; *NS*, non-statistically significant. *B*, 3F4-HEK293 cells were transiently transfected with ERK1, M1R, and ADAM17$_{wt}$ or ADAM17$_{T735A}$ cDNAs. Twenty-four hours after transfection cells were treated with (+) or without (−) PDBu (1 μM) or carbachol (100 μM). N1 secretion, PrP^c, ADAM17, HA-tagged ERK1, and M1R and tubulin immunoreactivities were measured as described previously. *Bars* correspond to densitometric analyses of N1 immunoprecipitation normalized by PrP^c expression and are expressed as a percentage of control (non-treated ADAM17$_{wt}$ transfected cells, *black bar*) taken as 100 and represent the mean ± S.E. of three independent experiments. *, $p < 0.001$; *NS*, non-statistically significant. *C*, 3F4-HEK293 cells were transiently transfected with empty pcDNA3 (*DNA3*) or constitutively active MEK kinase (*CAM*) with ADAM17$_{wt}$ or ADAM17$_{T735A}$. N1, PrP^c, ADAM17, HA-tagged CAM, and tubulin immunoreactivities were measured as described previously. *Bars* correspond to densitometric analyses of N1 immunoprecipitation and are expressed as a percentage of control (ADAM17$_{wt}$, DNA3-transfected cells, *black bar*) taken as 100 and represent the mean ± S.E. of three independent experiments. *, $p < 0.05$; **, $p < 0.001$; *NS*, non-statistically significant.

production (Fig. 6*C*, *left panel*) in agreement with the phenotype observed in ADAM17$^{-/-}$ cells (8). Moreover, we are able to partially recover PDBu- and carbachol-stimulated N1 production after transient transfection of wild-type ERK1 cDNA in ERK1-deficient MEFs (Fig. 6*C*, *right panel*). However, the very low levels of endogenous N1 secreted by ERK1-deficient cells due to low PrP^c expression in these fibroblasts and thus, the difficulty to visualize any modification in N1 production led us to confirm the loss of regulated PrP^c processing in ERK1$^{-/-}$ MEFs after transient transfection of PrP^c. As observed with endogenous N1, unlike wild-type fibroblasts, PrP^c-transfected ERK1$^{-/-}$ cells do not respond to carbachol stimulation (Fig. 6*D*). Importantly, similar results are obtained when cells are stimulated with PDBu (data not shown). In line with the latter results, carbachol-induced N1 secretion is blocked by the two MEK inhibitors PD098059 and Uo126 in wild-type but not ERK1$^{-/-}$ cells (Fig. 6*E*).

Besides the above described influence of ERK1 on N1 production, an additional feature concerned the consistent decrease of endogenous PrP^c-like immunoreactivity triggered by ERK1 deficiency (Fig. 6, *A* and *C*, *left panel*). This decrease is opposite to the augmentation of PrP^c expression observed in ERK1-transfected carbachol-treated M1R/3F4 HEK293 cells (Fig. 4*A*) and could suggest an additional putative role for ERK1 in the regulation of PrP^c expression. Therefore, one could envision that the N1 increase/reduction associated with ERK1 overexpression/ablation could be partly explained by upstream modulation of PrP^c expression. To specifically address the real impact of ERK1 on PrP^c metabolism, we measured α-secretase activity on intact cultured ERK1$^{-/-}$ and wild-type MEFs by means of the above described fluorimetric assay (14). Clearly, the BB3103-sensitive hydrolysis of the JMV2770 fluorimetric substrate was strongly affected in intact ERK1$^{-/-}$ MEFs when compared with wild-type cells (Fig. 6*B*) reflecting a direct involvement of this kinase in the regulation of the α-secretase processing of PrP^c. However, it was of importance to assess whether and how ERK1 could exert an effect on PrP^c expression besides its genuine influence on PrP^c processing.

We first confirmed that, *in vitro*, ERK1 deficiency triggered a 50% decrease in PrP^c immunoreactivity when compared with

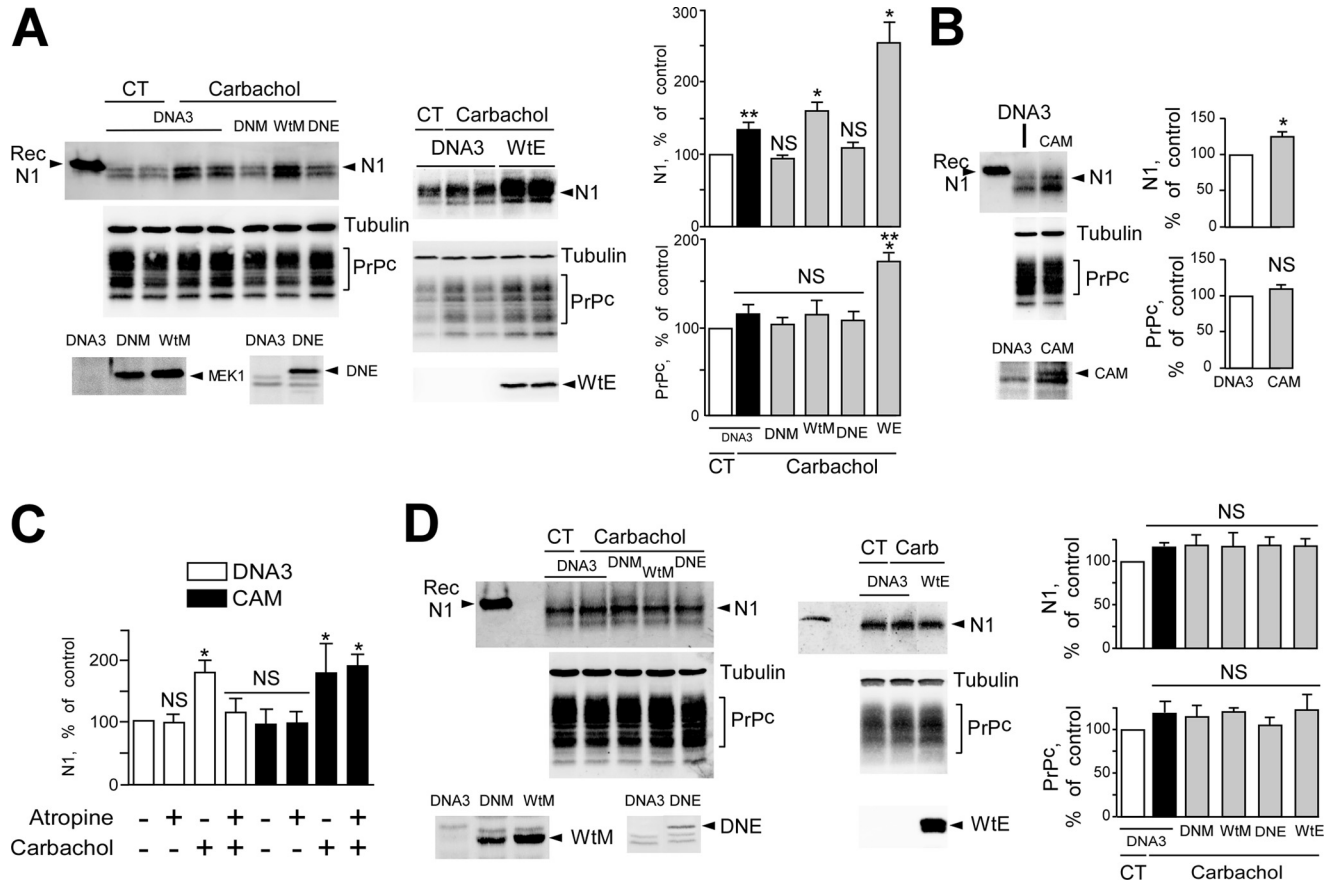

FIGURE 4. **Wild-type, dominant-negative, or constitutively active ERK1 or MEK1 modulate carbachol-dependent N1 secretion.** *A*, M1R-HEK293 cells were transiently transfected with Mo3F4 PrP^c cDNA together with empty pcDNA3 (*DNA3*) or with pcDNA3 encoding wild-type ERK1 or MEK1 (*WtE* or *WtM*), dominant-negative ERK1 (*DNE*) or MEK1 (*DNM*) as indicated. Twenty-four hours after transfection, cells were incubated for 8 h with 1 ml of DMEM in the absence (*CT*) or presence of carbachol (100 μM), then media were taken out and N1 was immunoprecipitated and detected by 16.5% Tris/Tricine SDS-PAGE and Western blotting with the SAF32 antibody as described under "Experimental Procedures." Recombinant N1 peptide (*Rec N1*) was used as a standard. PrP^c, tubulin, and HA-tagged WtE, WtM, DNE, and DNM were analyzed as described under "Experimental Procedures." *Bars* correspond to densitometric analyses and are expressed as a percentage of control (*white bars*, non-stimulated cells co-transfected with Mo3F4 PrP^c cDNA and pcDNA3) taken as 100 and represent the mean ± S.E. of nine independent experiments. *, $p < 0.05$; **, $p < 0.005$; ***, $p < 0.0005$; *NS*, non-statistically significant. *B* and *C*, M1R-HEK293 cells were co-transfected with Mo3F4 PrP^c cDNA and empty vector (*DNA3*) or pcDNA3 encoding constitutively active MEK1 (*CAM*). Twenty-four hours after transfection, cells were incubated for 8 h with 1 ml of DMEM without (*B*) or with 100 μM carbachol, 10 μM atropine, or a combination of both (*C*). Collected media and cell lysates were assayed for their N1, PrP^c, tubulin, and HA-tagged CAM immunoreactivities as described above. *Bars* correspond to densitometric analyses and are expressed as a percentage of control (non-treated cells co-transfected with Mo3F4 PrP^c and pcDNA3) taken as 100 and represent the mean ± S.E. of nine independent experiments. *, $p < 0.005$; *NS*, non-statistically significant. *D*, 3F4-HEK293 cells were transiently transfected with empty pcDNA3 (*DNA3*) or with WtM, WtE, DNE, or DNM cDNA as indicated and treated as in *A*. N1, PrP^c, tubulin, and HA-tagged WtM, WtE, DNE, or DNM were measured as described in *A*. *Bars* correspond to densitometric analyses and are expressed as a percentage of control (*white bars*, non-stimulated cells transfected with pcDNA3) taken as 100 and represent the mean ± S.E. of six independent experiments. *NS*, non-statistically significant.

wild-type cells (Fig. 7*A*, *left panel*). This effect was specific because the levels of disintegrins ADAM9, ADAM10, and ADAM17 were not affected in ERK1$^{-/-}$ cells (Fig. 7*A*, *right panel*). Finally, we took advantage of ERK1 knock-out mice (17) to determine whether ERK1 could control PrP^c expression *in vivo* in mouse brain. Indeed, ERK1-deficient mice show statistically significant reduction of cerebral expression of PrP^c compared with wild-type animals (Fig. 7*B*).

ERK1 Positively Controls PrP^c Expression at a Transcriptional Level—It is well established that ERK1/2 can modulate the transcription of several genes (see Ref. 31 for review). We therefore examined the possibility that ERK1 could modulate PrP^c at a transcriptional level. Four lines of data suggest that it is indeed the case. First, transactivation of the human PrP^c promoter is significantly impaired by ERK1 depletion (Fig. 8*A*). Second, ERK1 deficiency lowers PrP^c mRNA levels as shown by quantitative real-time PCR (Fig. 8*B*). Third, transient transfection of CA MEK1cDNA in M1R HEK293 cells significantly enhances PrP^c promoter transactivation (Fig. 8*C*, *gray bar*) and PrP^c mRNA levels (Fig. 8*D*, *gray bar*). Fourth, DN-ERK1 or DN-MEK1 expressions reduce both PrP^c promoter transactivation and mRNA levels (Fig. 8, *C* and *D*, *black bars*).

To clearly dissociate the effects of ERK1 on the modulations of PrP^c cleavage and expression, we examined the ability of ERK/MEK to increase PrP^c expression in MEFs ADAM17$^{-/-}$ cells. In both MEFs ADAM17$^{-/-}$ and control cells (see immunoreactivities in Fig. 9*A*), as described previously, the transient transfection of CA-MEK1 increases PrP^c expression (Fig. 9*A*) and PrP^c promoter transactivation (Fig. 9*B*). Furthermore, in BB3103-treated mock- and CA-MEK-transfected cells where ADAM17 activity was virtually abolished (Fig. 9*C*), PrP^c promoter transactivation triggered by CA-MEK1 transfection remained unaffected by the pharmacological inhibition of α-secretase activity (Fig. 9*D*). This set of data clearly shows that

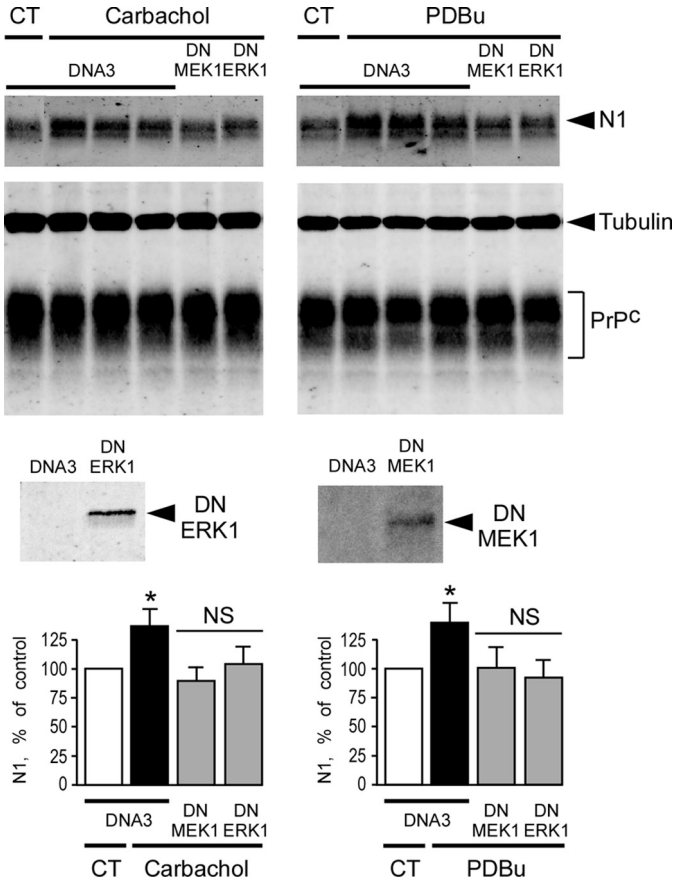

FIGURE 5. **Dominant-negative ERK1 and MEK1 abrogate PDBu- and carbachol-stimulated endogenous production of N1 in mouse primary cultured neurons.** Primary neurons were prepared from 14-day-old mouse embryos and cultured for 4 days, then cells were transfected with empty pcDNA3 (*DNA3*) or with DN-ERK1 or DN-MEK1 cDNAs as indicated. Twenty-four hours after transfection, cells were incubated for 8 h with 1 ml of DMEM in the absence (*CT*) or presence of PDBU (1 μM) (*right panel*) or carbachol (100 μM) (*left panel*). The media were taken out and N1 was immunoprecipitated and Western blotted as described under "Experimental Procedures." PrP^c, tubulin, and HA-tagged ERK1 and MEK1 contents were detected in cell lysates by separating 50 μg of proteins by 12% glycine SDS-PAGE as described under "Experimental Procedures." *Bars* correspond to densitometric analyses of N1 and are expressed as a percentage of control (non-stimulated cells transfected with pcDNA3) taken as 100 and represent the mean ± S.E. of six independent experiments. *, $p < 0.0001$; *NS*, non-statistically significant. Note that the *upper left N1 blot* was spliced for a clearer data presentation but that all the lanes derive from the same blot.

ERK controls PrP^c promoter transactivation independently of its effect on ADAM17 and therefore, that ERK1-associated modulation of ADAM17-increased N1 production could not be accounted for by the sole increase in the expression of its PrP^c precursor.

We then examined by which mechanisms ERK1 could control PrP^c promoter transactivation, mRNA, and protein levels. The role of ERK1 in the regulation of gene transcription has been well documented. ERK1/2 mainly operates through two main mechanisms, *i.e.* the phosphorylation of Sp1 that binds to GC box elements or via the phosphorylation of c-Fos that associates with phosphorylated c-Jun to form an AP-1 active transcription factor that interacts with one specific AP-1-recognizing sequence (see Ref. 31 for review). *In silico* examination of the PrP^c promoter revealed such Sp1-related GC box elements at position −1384/−1378 and one AP-1 consensus binding site at position −267/−260 (Fig. 10*A*). We first examined whether these two putative ERK1/2-regulated sites indeed behaved as PrP^c transcription activators by means of deletion analysis of the 5′ PrP^c promoter region (25). Deletion of the Sp1 binding site does not affect luciferase activity (compare −1543 and −1303 constructs; Fig. 10*B*), whereas removal of the AP-1 consensus binding sequence by mutagenesis strongly impairs PrP^c promoter transactivation in M1R HEK293 (compare −284 and −131 constructs; Fig. 10*B*). This suggests that ERK1/2 likely regulates PrP^c transcription through binding of AP-1 to the −267/−260 region of the PrP^c promoter. To further validate this hypothesis, we mutated the AP-1 responsive element of the full-length PrP^c promoter (TGACTCA → TAAaTCA) (−1543mut). Measurement of luciferase activity after transient transfections of −1543mut, −1543wt, or the −131 construct in M1R HEK293 and fibroblasts showed that the inactivating mutation led to a significant decrease of PrP^c transactivation when compared with the wild-type construct (Fig. 10*C*). Because the point mutation failed to mimic the extent of the effect of the entire deletion encompassing the AP-1 consensus binding site (compare −1543mut with −131; Fig. 10*C*), it is likely that the −284/−131 region of the PrP^c promoter is under the positive control of additional transcription factors.

DISCUSSION

Although the importance of the cellular prion protein in the development of TSEs has been extensively documented (see Ref. 1 for review), less is known concerning the physiological roles fulfilled by this protein. Because PrP^c knock-out mice are viable and fertile with no apparent dysfunction (32), it has long been thought that PrP^c does not participate in any vital physiological process. However, subsequent studies showed that PrP^c could contribute to various biological functions such as lymphocyte activation, cell adhesion, synaptic transmission, and apoptosis (see Ref. 3 for review). Noteworthy, PrP^c is subjected to a physiological proteolytic breakdown at its 111/112 peptide bond (4). There exist strong evidence that disintegrins ADAM10 and ADAM17 are responsible for the constitutive and PKC-regulated pathway (8, 14), respectively. It should be noted, however, that a few studies failed to find evidence for an involvement of ADAM proteases on PrP^c processing but this discrepancy may be likely explained by distinct experimental conditions in which recombinant soluble enzyme were used or because only constitutive processing was examined (33, 34).

This proteolytic event further complicates our understanding of PrP^c-related biological effects and raises the question whether this proteolytic attack represents a degradation process aimed at clearing full-length PrP^c or indeed illustrates a maturation step yielding biologically active metabolites. Concerning the C1 fragment, we previously showed that its overexpression potentiates staurosporine-induced apoptosis *in vitro* (23) as PrP^c does (35–37). As far as the N1 fragment is concerned, the first indirect demonstration of an N1-related function was first brought by *in vivo* studies showing that transgenic mice expressing N-terminal-truncated PrP^c constructs displayed exacerbated neurodegeneration and that this phenotype strictly requires the depletion of the 32-121 N-terminal sequence, thereby suggesting a putative N1-associated neuro-

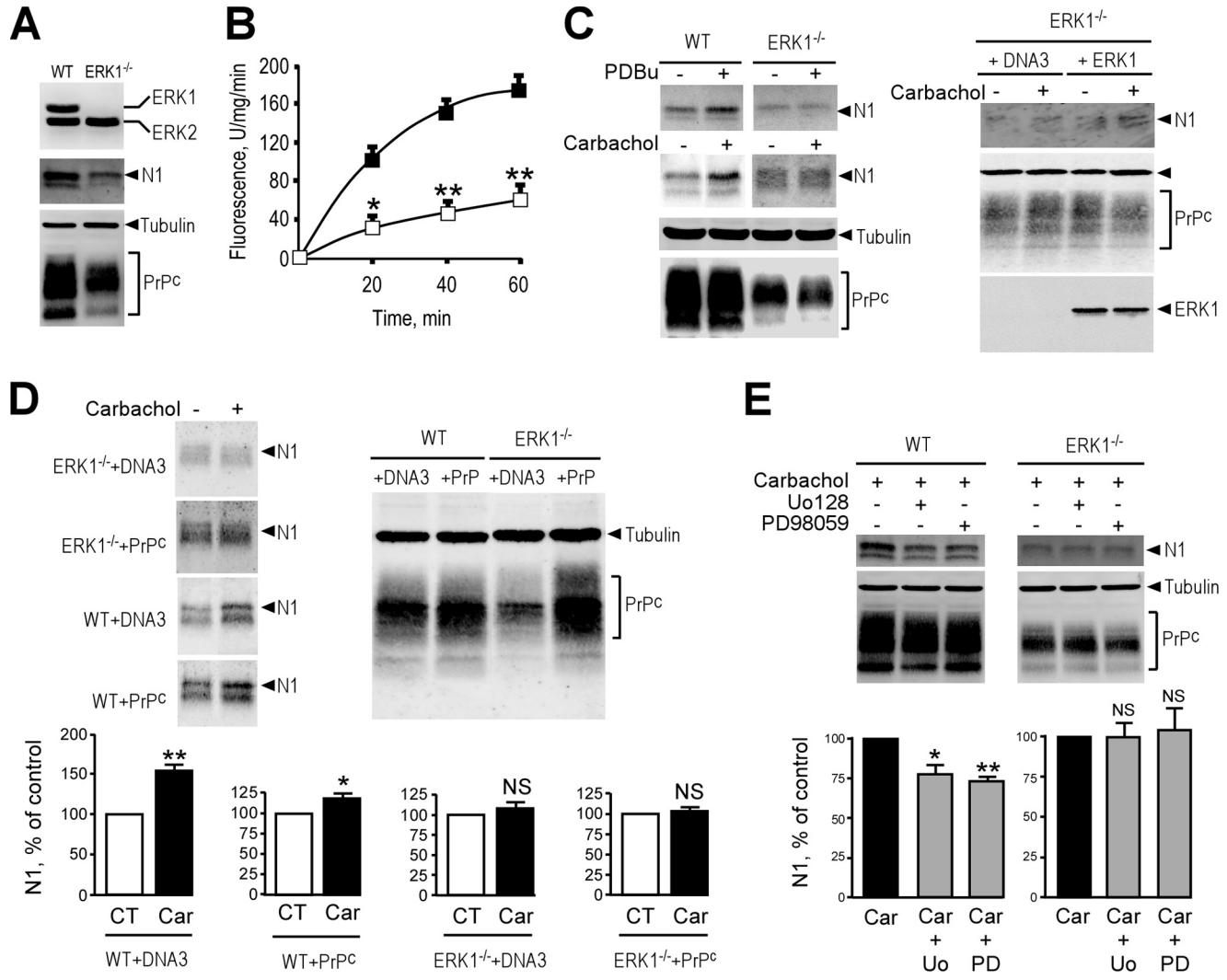

FIGURE 6. **ERK1 deficiency impairs PDBu- and carbachol-stimulated recovery of endogenous N1, reduces disintegrin activity, and lowers PrP^c expression.** *A*, wild-type (*WT*) or ERK1-deficient (*ERK1*$^{-/-}$) MEFs were incubated for 8 h with 1 ml of DMEM, then N1 was immunoprecipitated and analyzed by 16.5% Tris/Tricine electrophoresis and Western blot as described under "Experimental Procedures." ERK1/ERK2, PrP^c, and tubulin immunoreactivities were analyzed as described under "Experimental Procedures." *B*, plated WT (*black squares*) or ERK1$^{-/-}$ MEFs (*white squares*) were monitored for their JMV2770-hydrolyzing activity by fluorimetry according to the procedure described under "Experimental Procedures." *Bars* correspond to the BB3103-sensitive JMV2770-hydrolyzing activities and are the mean ± S.E. of four independent experiments. *, $p < 0.005$; **, $p < 0.001$. *C*, *left panel*, N1 secretion as well as PrP^c and tubulin immunoreactivities were measured in WT and ERK1$^{-/-}$ MEFs following an 8-h incubation in the absence (−) or presence (+) of PDBu (1 μM) or carbachol (100 μM). *Right panel*, complementation experiments were carried out in ERK1$^{-/-}$ MEFs by transient transfection with either empty pcDNA3 vector (*DNA3*) or ERK1 cDNA. Twenty-four hours after transfection, cells were incubated for 8 h with 1 ml of DMEM in the absence (−) or presence (+) of carbachol (100 μM) and N1 recovery, PrP^c, and tubulin immunoreactivities were assessed as described under "Experimental Procedures." *D*, WT or ERK1$^{-/-}$ MEFs were transiently transfected with either empty pcDNA3 vector (*DNA3*) or with Mo3F4 PrP^c cDNA (*PrP*^{c}). Twenty-four hours after transfection, cells were treated (+) or not (−) with carbachol (*Car*, 100 μM) and N1 was immunoprecipitated and analyzed as described under "Experimental Procedures" (*upper left panel*). PrP^c transfection efficacy in both cell lines was verified by Western blot (*upper right panel*). *Bars* correspond to densitometric analyses of N1 immunoreactivities in the indicated cell lines and transfection conditions and are expressed as a percentage of control (*CT*, non-stimulated cells) taken as 100 and represent the mean ± S.E. of eight independent experiments. *, $p < 0.005$; **, $p < 0.0001$. *E*, WT or ERK1$^{-/-}$ fibroblasts were pretreated (+) or not (−) for 1 h with Uo126 (*Uo*, 10 μM) or PD98059 (*PD*, 20 μM) and incubated for 8 h in the presence of carbachol (100 μM). Secreted N1 as well as PrP^c and tubulin immunoreactivities in lysates were analyzed as described under "Experimental Procedures." *Bars* correspond to densitometric analyses of N1 immunoreactivities expressed as a percentage of control (carbachol-stimulated cells in the absence of inhibitors) taken as 100 and represent the mean ± S.E. of three independent determinations. *, $p < 0.05$; **, $p < 0.0001$.

protective effect (38–40). We brought the definitive and direct proof that N1 indeed conveys neuroprotection by showing that treatment with the recombinant N1 peptide or stimulation of N1 production by muscarinic agonists invariably protect cells from hypoxia-induced p53-dependent apoptosis and ischemia *in vitro* and *in vivo* (41). Noteworthy, it has been very recently established that ablation of neuronal PrP^c triggers a chronic demyelinating polyneuropathy due to impaired peripheral myelin maintenance (42). This was an additional demonstration of a PrP^c-associated pathology of the peripheral nervous system unrelated to TSEs. Interestingly, chronic demyelinating polyneuropathy can be rescued by PrP^c variants that undergo disintegrin-mediated proteolytic processing at the 111/112 site but not by cleavage-resistant variants. Therefore, the N1 and/or C1 fragments derived from the physiological processing of PrP^c are essential for myelin maintenance (42). Altogether, and because we established that the N1-associated neuroprotective function was dominant over the C1-mediated toxic effect (41), these data suggests that up-regulating α-secretase processing of PrP^c could convey beneficial effects in normal conditions as

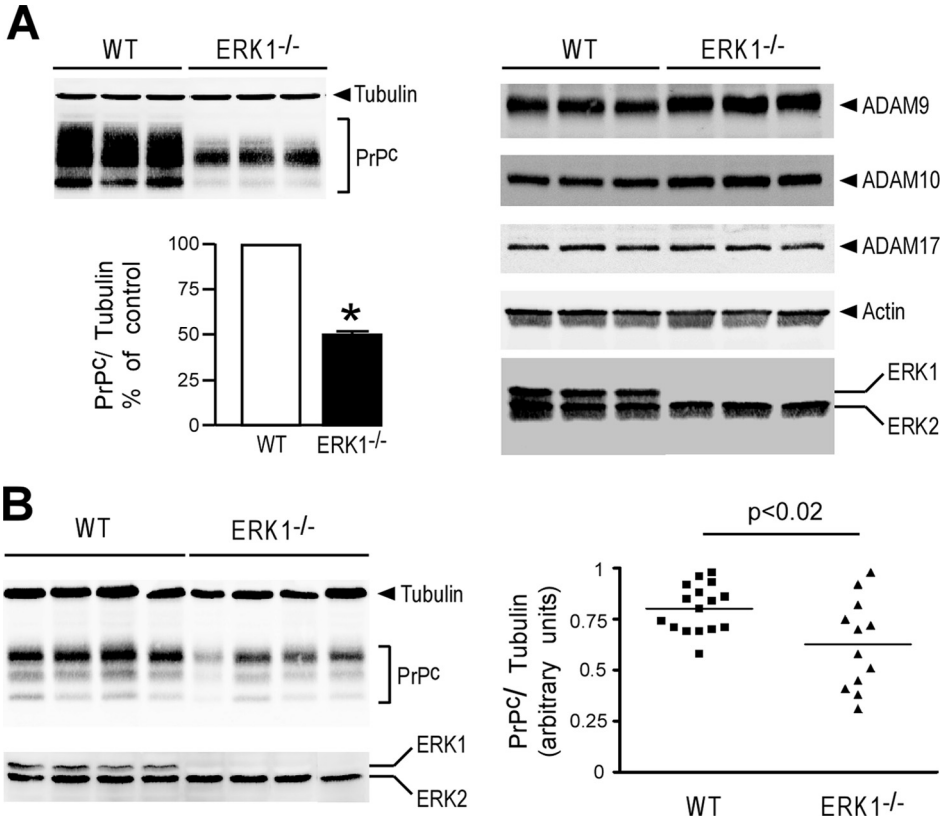

FIGURE 7. **ERK1 controls PrP^c expression *in vitro* and *in vivo*.** *A*, PrP^c (*left panel*), ADAM9, ADAM10, ADAM17, actin, and ERK1/2 (*right panels*) immunoreactivities were measured in WT and ERK1$^{-/-}$ MEF cell homogenates by SDS-PAGE and Western blot analysis of 50 μg of proteins as described under "Experimental Procedures." *Bars* correspond to densitometric analyses of PrP^c immunoreactivity (normalized with tubulin) expressed as a percentage of control (WT cells) taken as 100 and represent the mean ± S.E. of 12 independent determinations. *, $p < 0.0001$. *B*, PrP^c, tubulin, and ERK immunoreactivities in brain homogenates prepared from 7-week-old wild-type (*WT*) and ERK1$^{-/-}$ mice analyzed as described under "Experimental Procedures" were determined. The *right panel* shows densitometric analyses of PrP^c (normalized by tubulin levels) in brains of 16 wild-type mice and 12 ERK1$^{-/-}$ animals.

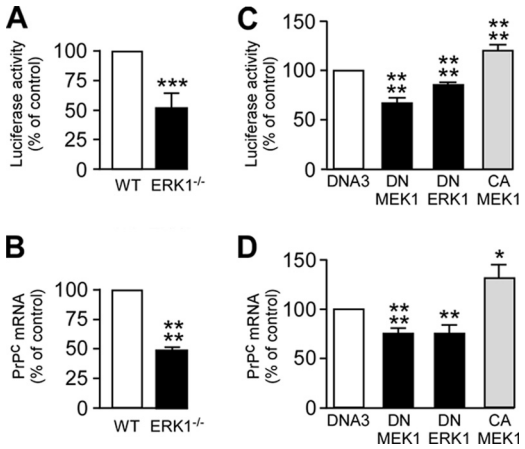

FIGURE 8. **ERK1 regulates PrP^c expression at a transcriptional level.** *A* and *B*, PrP^c promoter transactivation (*A*) and mRNA levels (*B*) were measured as described under "Experimental Procedures" in WT and ERK1$^{-/-}$ MEFs. *Black bars* represent the ratios of luciferase/β-galactosidase activities normalized by protein concentrations (*A*) or mRNA levels measured by real-time PCR (*B*) and are expressed as a percentage of control (WT cells) taken as 100 and are the mean ± S.E. of six independent determinations. *C* and *D*, M1R-HEK293 cells were transiently transfected with either empty vector (*DNA3*) or with DN-ERK1, DN-MEK1 (*black bars*), or CA-MEK1 (*gray bars*) cDNAs. After a 36-h period in the presence of carbachol (100 μM), PrP^c promoter transactivation (*C*) and mRNA levels (*D*) were analyzed as described under "Experimental Procedures." *Bars* correspond to the ratios of luciferase/β-galactosidase activities normalized by protein concentrations (*C*) or mRNA levels measured by real-time PCR (*D*), and are expressed as a percentage of control (pcDNA3-transfected cells) taken as 100 and are the mean ± S.E. of nine independent determinations. *, $p < 0.05$; **, $p < 0.01$; ***, $p < 0.001$; ****, $p < 0.0001$.

well as in pathological conditions unrelated to prion diseases. Therefore, a possible track would be to activate the PKC-regulated α-secretase hydrolysis of PrP^c at the 111/112 peptide bond. Phosphorylation of ADAM17 on its intracytoplasmic threonine residue at position 735 is necessary to activate this pathway (11). This amino acid is embedded in a consensus phosphorylation site targeted by ERK1/2. We therefore examined whether this kinase was directly responsible for ADAM17 activation through Thr-735 phosphorylation and, thereby, could act as a direct and functional activator of PKC-regulated α-secretase processing of PrP^c. Four lines of data indicate that it is indeed the case. First, inhibition of MEK, a kinase occurring upstream in the MEK/ERK signaling cascade reduces α-secretase JMV2770-hydrolyzing activity and drastically impairs N1 secretion and ADAM17 phosphorylation. Second, transient overexpression of wild-type or constitutively active forms of these two kinases in both human cells and murine primary neurons activate PDBu- and carbachol-dependent N1 production, whereas dominant-negative kinases reduce the recovery of N1 in the conditioned medium. Third, ERK1 deletion impairs PKC-regulated α-secretase activity and abolishes PDBu- and carbachol-dependent N1 secretion. Fourth, ERK1 cDNA transfection in ERK1$^{-/-}$ cells rescues carbachol-dependent secretion of N1. Overall, we propose that the M1/M3 muscarinic receptors activation triggers ADAM17-dependent processing of PrP^c at the 111/112 site after initiating the MEK/ERK path-

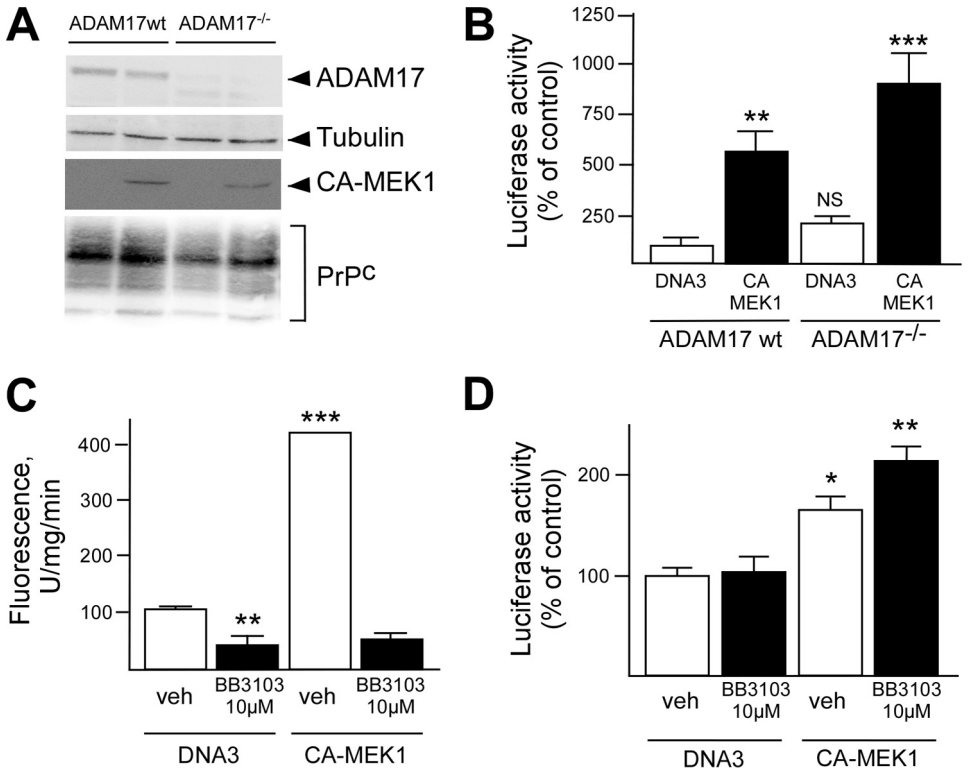

FIGURE 9. **ADAM17 deficiency and ADAM17 inhibitor do not affect ERK1-mediated regulation of PrP^c expression and promoter transactivation.** *A*, WT or ADAM17$^{-/-}$ MEFs were transiently transfected with pcDNA3 empty vector (*DNA3*) or pcDNA3 encoding constitutively active MEK1 (*CA-MEK1*). Twenty-four hours after transfection cells were collected, lysed as described under "Experimental Procedures," and analyzed by 8 or 12% glycine SDS-PAGE and Western blotting using antibodies specifically directed against ADAM17, HA-tagged CA-MEK, PrP^c, or tubulin. *B*, WT or ADAM17$^{-/-}$ MEFs were transiently co-transfected with wild-type full-length PrP^c promoter-luciferase construct (−1543 wt) and either DNA3 or CA-MEK1 cDNAs. Thirty-six hours after transfection, luciferase activity was measured as described under "Experimental Procedures." Values are expressed as percentage of control (MEFs WT transfected with −1543 wt and DNA3) taken as 100 and are the mean ± S.E. of 12 independent determinations. *C* and *D*, ADAM17-HEK293 cells were transiently co-transfected with −1543wt, DNA3, or CA-MEK1 cDNAs. Twenty-four hours after transfection, cells were treated or not (vehicle, *veh*) with BB3103 (10 μM) and monitored for their JMV2770-hydrolyzing activities as described under "Experimental Procedures." *C*, values are expressed in fluorescence units per min/mg of protein. Thirty-six hours after transfection, luciferase activity was measured (*D*) as described under "Experimental Procedures." Values are expressed as percentage of control (cells transfected with −1543wt and DNA3 without BB3103 treatment) taken as 100 and are the mean ± S.E. of six (*C*) or four (*D*) independent determinations. *, $p < 0.05$; **, $p < 0.01$; ***, $p < 0.001$.

way depicted in *green* in Fig. 11. ERK1-mediated control of PrP^c processing is not the only example of such an ERK1-controlled proteolytic conversion. Thus, the neurotrophin receptor TrkA shedding is also stimulated through an ERK1-dependent phosphorylation of ADAM17 at its Thr-735 in both *in vitro* assay and cultured cells (43). Moreover, this molecular event induces maturation and trafficking of ADAM17 to the plasma membrane thereby explaining the gain of activity of the ERK1-dependent threonine 735-phosphorylated ADAM17 form (44). However, this cascade is not ubiquitous because we recently demonstrated that α-secretase-regulated processing of β-amyloid precursor protein indeed involved ADAM17 and PKCs but in an ERK-1-independent manner (45).

Interestingly, PrP^c-like immunoreactivity was significantly reduced in ERK1$^{-/-}$ MEFs. This led us to examine the putative involvement of ERK1 in the regulation of PrP^c expression. We established that the observed ERK1-dependent reduction in PrP^c immunoreactivity results from a direct effect on PrP^c transcription. First, ERK1 depletion lowers PrP^c promoter transactivation and mRNA levels. Second, transient expression of dominant-negative forms of ERK1 or MEK1 significantly reduced PrP^c promoter activation and mRNA levels in HEK293 cells. Third, constitutively active MEK1 triggers the opposite effect. How does ERK signaling modulate PrP^c promoter transactivation? Several clues came from molecular cloning and characterization of the human, bovine, and mouse *PRNP* gene (25, 26, 46, 47) that revealed consensus binding sequences for several transcription factors, namely Sp1, AP-1, AP-2, c-Rel, Nkx2–5, Ets-1, and NF-AT. Several of these putative effectors proved to be functional for modulating PrP^c transcription in pathophysiological situations such as Sp1-dependent control of copper homeostasis (48) or presenilin-dependent p53-mediated PrP^c apoptosis (49).

We clearly showed that transcription factor AP-1, but not Sp1, contributes, at least partly, to the ERK1-dependent control of PrP^c. Thus, cDNA constructs harboring various 5′ deletions indicate that the ablation of the promoter region containing the AP-1 binding site, but not Sp1-related GC box elements, strongly impaired PrP^c promoter transactivation. Accordingly, inactivating mutations of the AP-1 binding sequence in the full-length promoter significantly reduce its promoter transactivation in two different cell lines. However, the fact that the extent of inhibition triggered by the −284/−131 deletion was higher than that resulting from the AP-1 site mutation (55–70% compared with 30% inhibition, Fig. 10*C*), suggests that additional transcription factors, the binding sites of which would be

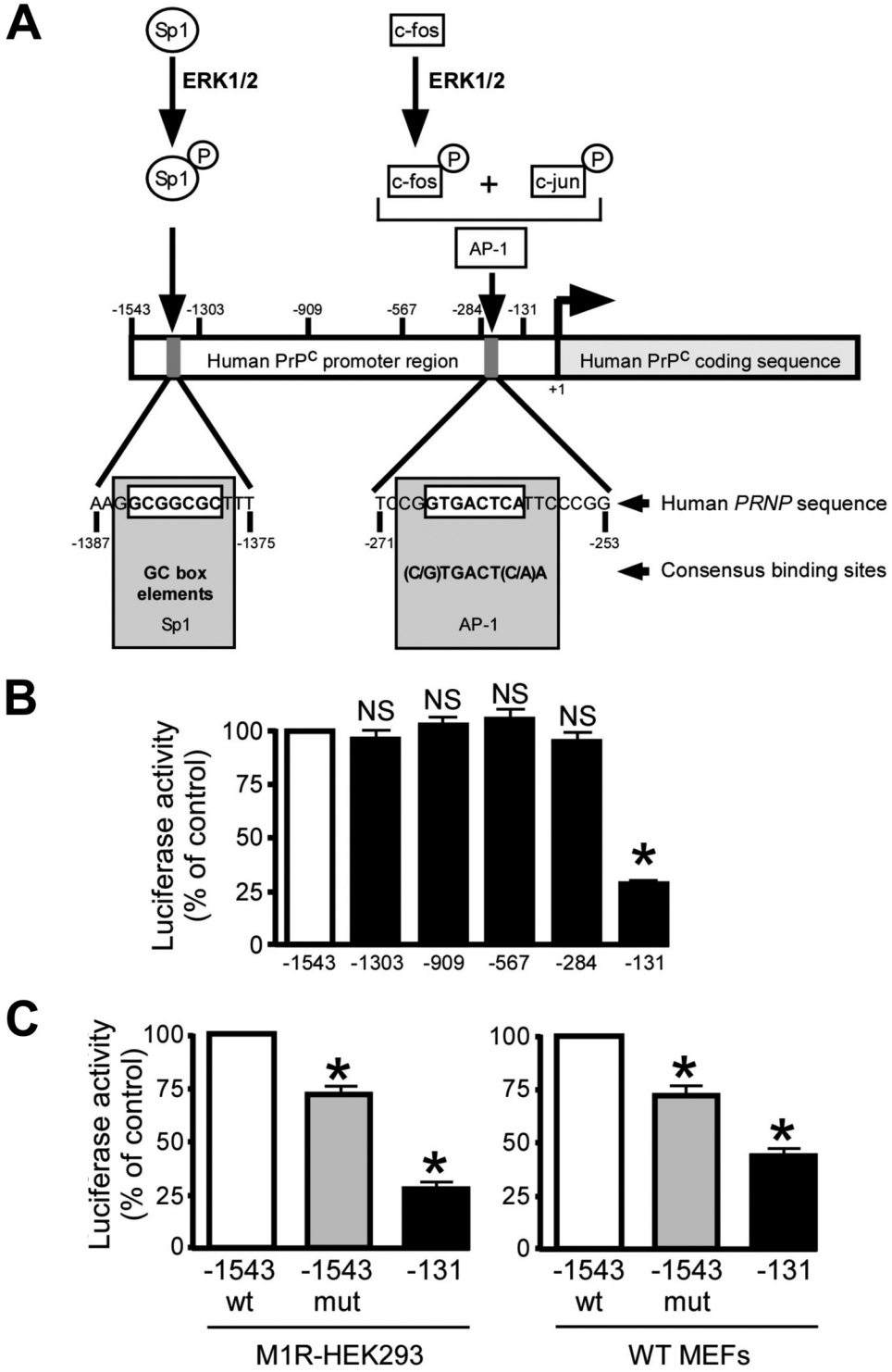

FIGURE 10. **Disruption of a putative AP1 responsive element of PrP^c promoter reduces ERK-regulated PrP^c promoter transactivation.** *A,* theoretical representation of activations of Sp1 and AP-1 by ERK1/2 and localization of two putative binding sites for Sp1 and AP-1 on the human PrP^c promoter region. *Gray boxes* show the regions of the human *PRNP* promoter harboring putative Sp1 and AP-1 responsive elements (*white boxes*) compared with their canonical consensus binding sequences. *B*, M1R-HEK293 cells were transiently transfected with the indicated human PrP^c promoter-luciferase constructs (the 5′ deletion mutant constructs of the PrP^c promoter region are indicated on the *abscissa* by their number of nucleotides and schematically localized on the *PRNP* promoter in *A*). Thirty-six hours after transfection, luciferase reporter activity was measured as described under "Experimental Procedures." *Bars* correspond to the ratios of luciferase/β-galactosidase activities (normalized by protein concentrations) expressed as a percentage of control (activity of the full-length −1543 promoter) taken as 100 and are the mean ± S.E. of nine independent determinations. *, $p < 0.001$; *NS*, non-statistically significant. *C*, M1R-HEK293 cells or WT MEFs were transiently transfected with wild-type full-length PrP^c promoter (−1543 wt, *white bars*), full-length PrP^c promoter mutated on its AP-1-binding site (−1543mut, *gray bars*), or with the AP-1 site-deleted construct (−131, *black bars*). Thirty-six hours after transfection, luciferase activity was measured as described under "Experimental Procedures." Values are expressed as a percentage of control (cells transfected with −1543wt) taken as 100 and are the mean ± S.E. of 12 independent determinations. *, $p < 0.001$.

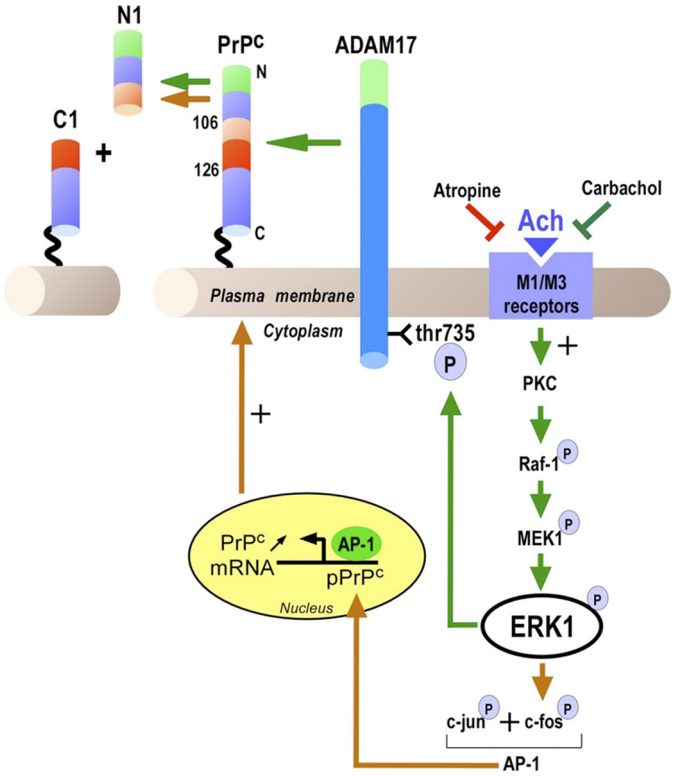

FIGURE 11. **Schematic representation of the dual ERK1-dependent impact on regulated processing and transcription of PrP^c.** Stimulation of M1/M3 muscarinic receptors triggers PKC-dependent activation of the MEK/ERK signaling pathway. Activated ERK1 then 1) directly phosphorylates ADAM17 on its intracytoplasmic threonine residue at position 735, thereby increasing ADAM17 activity, the processing of PrP^c at the 111/112 peptidyl bond, and the secretion of the neuroprotective N1 fragment; 2) increases PrP^c promoter transactivation and mRNA levels in an AP1-dependent manner. Mutational analysis indicates that AP-1 directly activates PrP^c transcription likely after formation of well documented ERK-1-dependent build-up with phosphorylation of c-Fos and its subsequent association with phospho-c-Jun (65). Therefore, under physiological conditions, ERK1 participates via two distinct processes (elevation of both substrate levels and enzyme activity) to an overall increase of the N1-associated neuroprotective phenotype.

located within position −284/−131, may also modulate PrP^c expression. It is noteworthy that binding sites for Ets-1, NF-AT, AP-2, YY1, and E4BP4 have been delineated in such a region (25, 50). Altogether, these data clearly established an important functional contribution of ERK1 and AP-1 in the positive control of PrP^c transcription (Fig. 11, *orange arrowheads*).

Because ERK increases both PrP^c expression and the production of its α-secretase-derived catabolite N1, one can question whether the increase of N1 is just the consequence of an upstream elevation of its precursor PrP^c or if ERK triggers dual and fully independent phenotypes. Close examination of some of the data indicates that the latter hypothesis is more likely. Thus, PDBu- and carbachol-stimulated N1 production is abolished in ERK-deficient cells, whereas PrP^c expression remains similar in treated and untreated null fibroblasts. This shows that agonist-dependent phosphorylation of ADAM17 and subsequent N1 production is impaired by ERK1 ablation, whereas reduction of PrP^c still stands. Second, ERK-1 rescues the carbachol-induced increase in N1 production without affecting PrP^c expression levels. This set of data reflects a clear discrimination between the two events that could be likely accounted for by distinct time frames for the two processes, with an early phase involving ADAM17 phosphorylation and enhanced PrP^c catabolism and a later phase needing a necessary delay to activate the transcriptional machinery.

Another interesting aspect of this work concerns the putative functional cross-talk between PrP^c and the MEK/ERK signaling pathway. Thus, PrP^c cross-linking or overexpression triggers ERK phosphorylation in neuronal and non-neuronal cells (51–55). Other studies established that the specific PrP^c ligand stress-inducible protein 1 (STI1) (56) likely accounts for PrP^c-dependent ERK phosphorylation in neurons and astrocytes (57–59). Therefore, the MEK/ERK cascade could self-stimulate its own signaling via the increase of PrP^c expression and thereby explain both ERK and PrP^c-related protective phenotypes documented in certain cell systems (3, 60, 61). Along with this hypothesis, one could envision that part of an ERK1-dependent PrP^c-associated antiapoptotic function could be mediated by an ERK-1-mediated increase in N1 because we recently characterized this catabolite as a neuroprotective factor both *in vitro* and *in vivo* (41).

In other cases, PrP^c has been shown to be toxic and trigger p53-dependent cell death (35–37). In this case, the ERK-1-mediated production of N1 could be seen as a cellular response to counterbalance PrP^c-mediated toxicity. This hypothesis seems to be supported by the observation that in cells overexpressing a PrP^c construct lacking the 32–134 amino-terminal sequence (that encompasses most of the N1 domain), ERK phosphorylation is still stimulated but leads to cell death, oxidative injury, and neurodegeneration (62–64). This could be due to the fact that whereas N-terminal-truncated PrP^c is increased, its neuroprotective counterpart N1 is lacking.

Overall, our study suggests that under normal conditions, ERK1 contributes to cell survival and neuroprotection through the augmentation of N1 secretion (41) via an increase in ADAM17 activity and PrP^c expression. It is likely that in pathological situations, N1 could temporarily compensate for the PrP scrapie-associated toxicity and cell death and thereby partly could explain the long asymptomatic time course of TSEs.

Acknowledgments—We thank Drs. J. Martinez and J. F. Hernandez (Montpellier, France) for kindly providing the fluorimetric substrate JMV2770 and Dr. Roy Black (Amgen Inc., Seattle, WA) for ADAM17 cDNA.

Note Added in Proof—We want to make clear that in some of the gels appearing in the article, lanes have been reorganized for purposes of clarity. All initial gels have been seen and reviewed by referees. All quantifications have been performed on initial gels before any rearrangements. As explained in the text, quantifications of data are means of several independent experiments, and gels are only representative of one of these experiments.

REFERENCES

1. Aguzzi, A., and Calella, A. M. (2009) *Physiol. Rev.* **89,** 1105–1152
2. Prusiner, S. B. (1998) *Proc. Natl. Acad. Sci. U.S.A.* **95,** 13363–13383

3. Linden, R., Martins, V. R., Prado, M. A., Cammarota, M., Izquierdo, I., and Brentani, R. R. (2008) *Physiol. Rev.* **88,** 673–728
4. Chen, S. G., Teplow, D. B., Parchi, P., Teller, J. K., Gambetti, P., and Autilio-Gambetti, L. (1995) *J. Biol. Chem.* **270,** 19173–19180
5. Forloni, G., Angeretti, N., Chiesa, R., Monzani, E., Salmona, M., Bugiani, O., and Tagliavini, F. (1993) *Nature* **362,** 543–546
6. Ettaiche, M., Pichot, R., Vincent, J. P., and Chabry, J. (2000) *J. Biol. Chem.* **275,** 36487–36490
7. Vincent, B., Paitel, E., Frobert, Y., Lehmann, S., Grassi, J., and Checler, F. (2000) *J. Biol. Chem.* **275,** 35612–35616
8. Vincent, B., Paitel, E., Saftig, P., Frobert, Y., Hartmann, D., de Strooper, B., Grassi, J., Lopez-Perez, E., and Checler, F. (2001) *J. Biol. Chem.* **276,** 37743–37746
9. Laffont-Proust, I., Faucheux, B. A., Hässig, R., Sazdovitch, V., Simon, S., Grassi, J., Hauw, J. J., Moya, K. L., and Haïk, S. (2005) *FEBS Lett.* **579,** 6333–6337
10. Cissé, M. A., Sunyach, C., Lefranc-Jullien, S., Postina, R., Vincent, B., and Checler, F. (2005) *J. Biol. Chem.* **280,** 40624–40631
11. Alfa Cissé, M., Sunyach, C., Slack, B. E., Fisher, A., Vincent, B., and Checler, F. (2007) *J. Neurosci.* **27,** 4083–4092
12. Alfa Cissé, M., Louis, K., Braun, U., Mari, B., Leitges, M., Slack, B. E., Fisher, A., Auberger, P., Checler, F., and Vincent, B. (2008) *Mol. Cell. Neurosci.* **39,** 400–410
13. Demart, S., Fournier, J. G., Creminon, C., Frobert, Y., Lamoury, F., Marce, D., Lasmézas, C., Dormont, D., Grassi, J., and Deslys, J. P. (1999) *Biochem. Biophys. Res. Commun.* **265,** 652–657
14. Cissé, M. A., Gandreuil, C., Hernandez, J. F., Martinez, J., Checler, F., and Vincent, B. (2006) *Biochem. Biophys. Res. Commun.* **347,** 254–260
15. Vincent, B., Beaudet, A., Dauch, P., Vincent, J. P., and Checler, F. (1996) *J. Neurosci.* **16,** 5049–5059
16. Nitsch, R. M., Slack, B. E., Wurtman, R. J., and Growdon, J. H. (1992) *Science* **258,** 304–307
17. Pagès, G., Guérin, S., Grall, D., Bonino, F., Smith, A., Anjuere, F., Auberger, P., and Pouysségur, J. (1999) *Science* **286,** 1374–1377
18. Pagès, G., Lenormand, P., L'Allemain, G., Chambard, J. C., Meloche, S., and Pouysségur, J. (1993) *Proc. Natl. Acad. Sci. U.S.A.* **90,** 8319–8323
19. Pagès, G., Brunet, A., L'Allemain, G., and Pouysségur, J. (1994) *EMBO J.* **13,** 3003–3010
20. Brunet, A., Pagès, G., and Pouysségur, J. (1994) *Oncogene* **9,** 3379–3387
21. Black, R. A., Rauch, C. T., Kozlosky, C. J., Peschon, J. J., Slack, J. L., Wolfson, M. F., Castner, B. J., Stocking, K. L., Reddy, P., Srinivasan, S., Nelson, N., Boiani, N., Schooley, K. A., Gerhart, M., Davis, R., Fitzner, J. N., Johnson, R. S., Paxton, R. J., March, C. J., and Cerretti, D. P. (1997) *Nature* **385,** 729–733
22. Bolton, D. C., Seligman, S. J., Bablanian, G., Windsor, D., Scala, L. J., Kim, K. S., Chen, C. M., Kascsak, R. J., and Bendheim, P. E. (1991) *J. Virol.* **65,** 3667–3675
23. Sunyach, C., Cisse, M. A., da Costa, C. A., Vincent, B., and Checler, F. (2007) *J. Biol. Chem.* **282,** 1956–1963
24. Bradford, M. M. (1976) *Anal. Biochem.* **72,** 248–254
25. Funke-Kaiser, H., Theis, S., Behrouzi, T., Thomas, A., Scheuch, K., Zollmann, F. S., Paterka, M., Paul, M., and Orzechowski, H. D. (2001) *J. Mol. Med.* **79,** 529–535
26. Mahal, S. P., Asante, E. A., Antoniou, M., and Collinge, J. (2001) *Gene* **268,** 105–114
27. Toullec, D., Pianetti, P., Coste, H., Bellevergue, P., Grand-Perret, T., Ajakane, M., Baudet, V., Boissin, P., Boursier, E., Loriolle, F., Duhamel, L., Charon, D., and Kirilovsky, J. (1991) *J. Biol. Chem.* **266,** 15771–15781
28. Favata, M. F., Horiuchi, K. Y., Manos, E. J., Daulerio, A. J., Stradley, D. A., Feeser, W. S., Van Dyk, D. E., Pitts, W. J., Earl, R. A., Hobbs, F., Copeland, R. A., Magolda, R. L., Scherle, P. A., and Trzaskos, J. M. (1998) *J. Biol. Chem.* **273,** 18623–18632
29. Dudley, D. T., Pang, L., Decker, S. J., Bridges, A. J., and Saltiel, A. R. (1995) *Proc. Natl. Acad. Sci. U.S.A.* **92,** 7686–7689
30. Peralta, E., Ashkenazi, A., Winslow, J. W., Ramachandran, J., and Capon, D. J. (1988) *Nature* **334,** 434–437
31. Boutros, T., Chevet, E., and Metrakos, P. (2008) *Pharmacol. Rev.* **60,** 261–310
32. Büeler, H., Fischer, M., Lang, Y., Bluethmann, H., Lipp, H. P., DeArmond, S. J., Prusiner, S. B., Aguet, M., and Weissmann, C. (1992) *Nature* **356,** 577–582
33. Taylor, D. R., Parkin, E. T., Cocklin, S. L., Ault, J. R., Ashcroft, A. E., Turner, A. J., and Hooper, N. M. (2009) *J. Biol. Chem.* **284,** 22590–22600
34. Endres, K., Mitteregger, G., Kojro, E., Kretzschmar, H., and Fahrenholz, F. (2009) *Neurobiol. Dis.* **36,** 233–241
35. Paitel, E., Alves da Costa, C., Vilette, D., Grassi, J., and Checler, F. (2002) *J. Neurochem.* **83,** 1208–1214
36. Paitel, E., Fahraeus, R., and Checler, F. (2003) *J. Biol. Chem.* **278,** 10061–10066
37. Paitel, E., Sunyach, C., Alves da Costa, C., Bourdon, J. C., Vincent, B., and Checler, F. (2004) *J. Biol. Chem.* **279,** 612–618
38. Shmerling, D., Hegyi, I., Fischer, M., Blättler, T., Brandner, S., Götz, J., Rülicke, T., Flechsig, E., Cozzio, A., von Mering, C., Hangartner, C., Aguzzi, A., and Weissmann, C. (1998) *Cell* **93,** 203–214
39. Radovanovic, I., Braun, N., Giger, O. T., Mertz, K., Miele, G., Prinz, M., Navarro, B., and Aguzzi, A. (2005) *J. Neurosci.* **25,** 4879–4888
40. Li, A., Barmada, S. J., Roth, K. A., and Harris, D. A. (2007) *J. Neurosci.* **27,** 852–859
41. Guillot-Sestier, M. V., Sunyach, C., Druon, C., Scarzello, S., and Checler, F. (2009) *J. Biol. Chem.* **284,** 35973–35986
42. Bremer, J., Baumann, F., Tiberi, C., Wessig, C., Fischer, H., Schwarz, P., Steele, A. D., Toyka, K. V., Nave, K. A., Weis, J., and Aguzzi, A. (2010) *Nat. Neurosci.* **13,** 310–318
43. Díaz-Rodríguez, E., Montero, J. C., Esparís-Ogando, A., Yuste, L., and Pandiella, A. (2002) *Mol. Biol. Cell* **13,** 2031–2044
44. Soond, S. M., Everson, B., Riches, D. W., and Murphy, G. (2005) *J. Cell Sci.* **118,** 2371–2380
45. Cissé, M., Braun, U., Leitges, M., Fisher, A., Pagès, G., Checler, F., and Vincent, B. (2011) *Mol. Cell. Neurosci.* **47,** 223–232
46. Westaway, D., Cooper, C., Turner, S., Da Costa, M., Carlson, G. A., and Prusiner, S. B. (1994) *Proc. Natl. Acad. Sci. U.S.A.* **91,** 6418–6422
47. Inoue, S., Tanaka, M., Horiuchi, M., Ishiguro, N., and Shinagawa, M. (1997) *J. Vet. Med. Sci.* **59,** 175–183
48. Bellingham, S. A., Coleman, L. A., Masters, C. L., Camakaris, J., and Hill, A. F. (2009) *J. Biol. Chem.* **284,** 1291–1301
49. Vincent, B., Sunyach, C., Orzechowski, H. D., St. Georges-Hyslop, P., and Checler, F. (2009) *J. Neurosci.* **29,** 6752–6760
50. Burgess, S. T., Shen, C., Ferguson, L. A., O'Neill, G. T., Docherty, K., Hunter, N., and Goldmann, W. (2009) *J. Biol. Chem.* **284,** 6716–6724
51. Schneider, B., Mutel, V., Pietri, M., Ermonval, M., Mouillet-Richard, S., and Kellermann, O. (2003) *Proc. Natl. Acad. Sci. U.S.A.* **100,** 13326–13331
52. Monnet, C., Gavard, J., Mège, R. M., and Sobel, A. (2004) *FEBS Lett.* **576,** 114–118
53. Stuermer, C. A., Langhorst, M. F., Wiechers, M. F., Legler, D. F., von Hanwehr, S. H., Guse, A. H., and Plattner, H. (2004) *FASEB J.* **18,** 1731–1733
54. Shyu, W. C., Lin, S. Z., Chiang, M. F., Ding, D. C., Li, K. W., Chen, S. F., Yang, H. I., and Li, H. (2005) *J. Neurosci.* **25,** 8967–8977
55. Pantera, B., Bini, C., Cirri, P., Paoli, P., Camici, G., Manao, G., and Caselli, A. (2009) *J. Neurochem.* **110,** 194–207
56. Zanata, S. M., Lopes, M. H., Mercadante, A. F., Hajj, G. N., Chiarini, L. B., Nomizo, R., Freitas, A. R., Cabral, A. L., Lee, K. S., Juliano, M. A., de Oliveira, E., Jachieri, S. G., Burlingame, A., Huang, L., Linden, R., Brentani, R. R., and Martins, V. R. (2002) *EMBO J.* **21,** 3307–3316
57. Lopes, M. H., Hajj, G. N., Muras, A. G., Mancini, G. L., Castro, R. M., Ribeiro, K. C., Brentani, R. R., Linden, R., and Martins, V. R. (2005) *J. Neurosci.* **25,** 11330–11339
58. Caetano, F. A., Lopes, M. H., Hajj, G. N., Machado, C. F., Arantes, C. P., Magalhães, A. C., Vieira Mde, P., Américo, T. A., Massensini, A. R., Priola, S. A., Vorberg, I., Gomez, M. V., Linden, R., Prado, V. F., Martins, V. R., and Prado, M. A. (2008) *J. Neurosci.* **28,** 6691–6702
59. Arantes, C., Nomizo, R., Lopes, M. H., Hajj, G. N., Lima, F. R., and Martins, V. R. (2009) *Glia* **57,** 1439–1449
60. Han, B. H., and Holtzman, D. M. (2000) *J. Neurosci.* **20,** 5775–5781

61. Cavanaugh, J. E., Jaumotte, J. D., Lakoski, J. M., and Zigmond, M. J. (2006) *J. Neurosci. Res* **84,** 1367–1375
62. Gavín, R., Braun, N., Nicolas, O., Parra, B., Ureña, J. M., Mingorance, A., Soriano, E., Torres, J. M., Aguzzi, A., and del Río, J. A. (2005) *FEBS Lett.* **579,** 4099–4106
63. Pietri, M., Caprini, A., Mouillet-Richard, S., Pradines, E., Ermonval, M., Grassi, J., Kellermann, O., and Schneider, B. (2006) *J. Biol. Chem.* **281,** 28470–28479
64. Nicolas, O., Gavín, R., Braun, N., Ureña, J. M., Fontana, X., Soriano, E., Aguzzi, A., and del Río, J. A. (2007) *FASEB J.* **21,** 3107–3117
65. Chiu, R., Boyle, W. J., Meek, J., Smeal, T., Hunter, T., and Karin, M. (1988) *Cell* **54,** 541–552